Mars Exploration Rovers – A New Standard for Interplanetary Navigation

Louis A. D'Amario and Michael M. Watkins
Jet Propulsion Laboratory, California Institute of Technology, Pasadena, California, 91109

The twin Mars Exploration Rovers, *Spirit* and *Opportunity*, arrived at Mars for landings respectively at Gusev Crater (on January 4, 2004) and Meridiani Planum (on January 25, 2004). During the development of the mission, the capability of the navigation system to deliver the landers within a particular accuracy played a major role in landing site selection. This process ultimately resulted in commitments to deliver each lander within a specified landing ellipse (about 70 km x 5 km) determined to be safe for landing and also judged to be scientifically interesting. Achieving atmospheric entry delivery accuracies consistent with this landing requirement necessitated significant improvements to the interplanetary navigation system used for MER. These improvements included new processes and software for orbit determination, aggressive, mission-critical use of interferometric ΔDOR tracking data, propulsive maneuver design, and entry, descent, and landing (EDL) trajectory simulation. Because these advances pressed the state –of –the art, innovative methods to verify the assumptions in the pre-launch covariance analyses were also developed. The actual achieved atmospheric entry accuracies for *Spirit* and *Opportunity* significantly bettered the requirements. At the navigation data cutoff for the TCM-5 final design, the orbit determination entry flight path angle (FPA) knowledge errors were ±0.028° (3σ) for *Spirit* and ±0.035° (3σ) for *Opportunity*. These FPA accuracies correspond to B-plane errors of less than 1 km, setting a new standard for interplanetary delivery accuracy. Because of the exceptionally accurate navigation performance, TCM-5 (E – 2 days) and TCM-6 (E – 4 hours) were canceled for both *Spirit* and *Opportunity*. The actual landing locations (determined from in-situ Doppler tracking between the MER rovers and the Mars Odyssey orbiter) differed from the target landing points by 10.1 km (downtrack) for *Spirit* and 24.6 km (downtrack) for *Opportunity*. The majority of the landing position offsets for both landers was primarily caused by variations in atmosphere and spacecraft aerodynamic modeling from what was predicted. The amount of the landing position offset caused by navigation-only errors was only 3.3 km (uptrack) for *Spirit* and 9.7 km (downtrack) for *Opportunity*.

I. Introduction

THE twin Mars Exploration Rovers, *Spirit* and *Opportunity*, were successfully launched on June 10, 2003[†], and July 8, 2003, from Cape Canaveral, Florida. *Spirit* (also known as MER-A) was targeted for a January 4, 2004, arrival at Mars. The arrival date for *Opportunity* (MER-B) was exactly three weeks later on January 25, 2004. The landing target for *Spirit* was within Gusev Crater. The target for *Opportunity* was in the Meridiani Planum region, essentially on the opposite side of Mars from Gusev. These landing sites were selected after much discussion, down-selection, and review, based largely on their being the most scientifically interesting sites that met landing safety requirements. Landing safety considerations included EDL constraints such as altitude, wind velocity and rock and slope distribution, but the most fundamental limitation in fact was the overall size of the landing ellipse itself. Since geomorphology, which leads to scientific interest, also often leads to significant topography (and hence slopes), the size of the landing ellipse governed how close to such interesting sites a safe landing area could be placed.

Early in the project development, the MER Navigation Team performed preliminary delivery accuracy analyses using "typical" and reasonable assumptions for the accuracy of the major error sources and for the amount and types of tracking data expected. Following discussion with the MER science team and site selection group, it was realized that pushing the envelope in navigation delivery accuracy could have high science payoff by opening

up additional landing sites with smaller safe zones. We therefore established a "No Margin Tiger Team", composed of experts in navigation and tracking systems, that embarked on an unprecedented in-depth review of all navigation error sources in an attempt to reduce the landing ellipses to the minimum size, while maintaining reasonable engineering margins. This effort was successful and resulted in Gusev Crater and other sites (ultimately not selected) emerging as feasible landing sites. The success of this activity was evidenced by the fact that at the Project Critical Design Review, the Principal Investigator indicated that the navigation improvements leading to smaller landing ellipses was the "best thing that had happened to the project".

The dimensions of the final target landing ellipses for both *Spirit* and *Opportunity* were quite small – i.e., on the order of 70 km (total downtrack) by 5 km (total crosstrack) at the 99% probability level. Since the MER landers followed essentially a ballistic trajectory in the atmosphere, in order to achieve landing within the target ellipse, precise control of inertial flight path angle (FPA) at atmospheric entry was required. The atmospheric entry interface point was defined to be at a Mars radius of 3522.2 km. The maximum allowable errors in FPA at TCM-5 (trajectory correction maneuver #5) at E – 2 days were $\pm 0.12°$ (3σ) for *Spirit* and $\pm 0.14°$ (3σ) for *Opportunity*. These errors are equivalent to a Mars B-plane accuracy of about ±3 km in the B-magnitude direction, which is roughly equivalent to the semi-minor axis (SMIA) of the Mars B-plane error ellipse.

Accomplishing the entry delivery accuracies quoted in the preceding paragraph necessitated significant improvements to the interplanetary navigation system used for MER. These improvements included new processes and software for orbit determination, propulsive maneuver design, entry, descent, and landing (EDL) trajectory simulation, and validation and verification methods. Orbit determination (OD) enhancements included reexamination of all assumptions used in the baseline OD filter to make them more realistic and eliminate unnecessary conservatism, inclusion of a campaign of frequent delta differenced one-way ranging (ΔDOR) measurements in the navigation baseline, development of a new OD scripting architecture for automated OD filter processing to enable computation and visualization of numerous solutions using varying OD filter assumptions (up to 50 cases in a single computer run), and development of new software for surface position determination using in-situ Doppler data between MER and the Mars Odyssey orbiter. New propulsive maneuver design processes were developed to rapidly evaluate maneuver options for TCM-1 in terms of maneuver epoch, landing target, and maneuver mode, and to evaluate and design propulsive maneuvers for TCMs 4, 5, and 6 to eliminate undesirable maneuver characteristics in terms of the path of the maneuver in the B-plane or on the surface. EDL trajectory simulation was enhanced in order to automate the process of atmospheric entry targeting to achieve a specified landing target, and new software was developed to visualize landing dispersions on Mars surface maps and to evaluate various statistical measures of landing site safety and various science-related factors.

The remainder of this paper focuses on the improvements made to system modeling and the orbit determination filter strategy, and a brief summary of the actual delivery performance. Detailed assessments of the MER navigation experience from launch through landed mission position determination can be found in Refs 1 – 9.

II. Navigation System Performance Assumptions

The navigation delivery is governed by two types of errors: dynamic modeling errors affecting the spacecraft trajectory and measurement modeling errors that limit the orbit determination process. Each of these areas has error sources that must be modeled correctly to accuracy predict system performance in covariance and Monte Carol analyses. The basic process followed by the Navigation Team and the Navigation and Mission Design Section was to investigate each area in detail, consult external experts where necessary, and lower the assumptions on errors to the "no margin" level generally corresponding to state-of-the-art performance or best-case statistics. The delivery accuracy in this case was compared with more conservative assumptions to bound performance.

The orbit determination process used a least-squares batch estimation filter. The filter minimized tracking data residuals over the data arc in order to estimate the state (position and velocity) of the spacecraft at a specified epoch (usually the start of the data arc) and any other parameters included in the estimation list. The filter also output the uncertainties in the estimated parameters. Parameters that are not estimated, but whose a priori uncertainties are incorporated in the results, are called consider parameters.

The OD filter configuration used just prior to launch for final OD covariance studies is shown in Table 1. These were the values used to downselect landing sites. During interplanetary cruise, prior to the final commitment to landing sites, the filter configuration was updated based on in-flight

experience in order to obtain the best possible validation of the filter assumptions. That configuration is presented in Table 2. These are generally more aggressive than in past missions, and require further discussion, presented below.

Table 1: OD filter configuration – pre-launch.

Error Source	Estimated?	A Priori Uncertainty (1σ)	Correlation Time	Update Time	Comments
2-way Doppler (mm/s)	–	0.075	–	–	~4.5 mHz
Range (m)	–	4	–	–	29 range units
ΔDOR (nrad)	–	4.5	–	–	0.12 ns
Epoch State					
Position (km)	✔	1000	–	–	
Velocity (km/s)	✔	1	–	–	
Solar Pressure					Sunlit area of spacecraft.
Area (%)	✔	5	–	–	
Specular & Diffuse Coefficients (%)	✔	10	–	–	
ACS Event ΔV (mm/s)					Every 8 days.
Line-of-Sight Comp.	✔	3	–	–	
Lateral Comp.	✔	3	–	–	
Normal Comp.	✔	3	–	–	
TCMs					MER-A, MER-B respectively
TCM-1	✔	422, 440	–	–	Spherical uncertainty (mm/s)
TCM-2	✔	17, 15	–	–	
TCM-3	✔	3, 5	–	–	TCM-4 at E - 8 days TCM-5 at E - 2 days TCM-6 at E - 6 hours
TCM-4	✔	3, 3	–	–	
TCM-5	✔	3, 3	–	–	5% (3σ) proportional error (per axis)
TCM-6	✔	7, 7	–	–	6 mm/s (3σ) fixed error (per axis)
Nongravitational Accelerations (km/s^2)	✔	2.0×10^{-12}	10 days	1 day	Spherical covariance; estimated daily (1 day batches).
Range Bias (m)	✔	2	0	Per pass	Estimated per pass.
Doppler Bias (mm/s)	✔	0.005	0	Per pass	Estimated per pass.
Mars & Earth Ephemerides	–	DE405+	–	–	
Station Locations (cm)	–	3	–	–	
Quasar Locations (nrad)	–	2	–	–	
Pole X, Y (cm)	✔	2 – 10	0	6 hours	*Use lower value up to 7 days before data cutoff; ramp up to higher value at data cutoff. (UT1: 0.256 ms = ~10 cm.)
UT1 (cm)	✔	2 – 10	0	6 hours	
Ionosphere – day (cm)	✔	55	0	6 hours	S-band values.
Ionosphere – night (cm)	✔	15	0	6 hours	
Troposphere – wet (cm)	✔	1	0	6 hours	
Troposphere – dry (cm)	✔	1	0	6 hours	

Navigation Data Types

The baseline radiometric data types used for orbit determination were two-way coherent Doppler, two-way coherent ranging, and ΔDOR measurements. Doppler and range are traditional data types derived from the coherent X-band radio link between the spacecraft and a receiver at a Deep Space Network (DSN) ground station. Doppler data provide a measurement of the line-of-sight spacecraft range rate based on Doppler frequency shift. Range data provide an estimate of the range to the spacecraft by measuring the round-trip light time of a radio signal between a DSN station and the spacecraft. For the pre-launch covariance analyses the Doppler accuracy assumption was improved to 4.5 mHz (1σ), which is equivalent to 0.075 mm/s (1σ) (lowered from the typical value of 0.1-0.2 mm/s). Range accuracy was assumed to be on the order of 4 m (1σ) for a 10-minute integration time based on link analysis by the MER telecom team.

Table 2: OD filter configuration – final approach.

Error Source	Estimated?	A Priori Uncertainty (1σ)	Correlation Time	Update Time	Comments
2-way Doppler (mm/s)	–	Weight by pass: ≥0.05	–	–	3.36 x RMS (60 sec) of pass-through residuals. (1.0 mm/s = ~0.056 Hz.)
Range (m)	–	Weight by pass: ≥0.14	–	–	2.22 x RMS of pass-through residuals. (1.0 m = ~7.0 RU.)
ΔDOR (nrad)	–	~3.2	–	–	0.085 ns
Epoch State					
Position (km)	✔	100,000	–	–	Effectively infinite.
Velocity (km/s)	✔	1.0	–	–	Effectively infinite.
Solar Pressure					
Specular Coefficients	✔	0.05	–	–	All components; 0.1 in normal units.
Diffuse Coefficients	✔	0.033			All components; 0.1 in normal units.
Solar Array Diffuse Coef.	✔	0.033	7 days	1 day	Correlation broken at turns.
ACS Event ΔV (mm/s)					
Line-of-Sight Comp.	✔	0.05, 0.1	–	–	MER-A & MER-B values respectively, based on results of ACS/NAV calibration. Location per current plan; all future events included.
Lateral Comp.	✔	0.05, 0.05	–	–	
Normal Comp.	✔	0.05, 0.05	–	–	
TCM-4					
Magnitude (%)	✔	1.67	–	–	Equivalent to 0.127 N.
Pointing (deg)	✔	0.5	–	–	Use 0.5 deg for both cone and clock.
Nongravitational Accelerations (km/s^2)	–	–	–	–	No longer used – accounted for in solar pressure uncertainties and modeling of ACS turns as discreet events.
Charged Particle Effects					
Delay (m)	✔	1.5	–	1 day	
Delay Rate (m/s)	✔	0.00005	–	1 day	Equivalent to ~4 meters per day
Range Bias (m)	✔	2	0	Per pass	Estimated per pass.
Doppler Bias (mm/s)	–	–	–	–	No longer used.
Mars & Earth Ephemerides	–	DE410	–	–	0.5 x DE405+; Mars RTN 1σ uncertainties: 9 m, 136 m, 442 m.
Station Locations (cm)	–	Per covariance.	–	–	Use latest updates to station locations and covariance.
Quasar Locations (nrad)	–	2	–	–	
Pole X, Y (cm)	✔	1, 4	2 days	6 hours	Use larger value for last 2 – 6 days per KEOF memo. (For UT1, 0.256 ms ⇒ ~10 cm.)
UT1 (cm)	✔	1.7, 9	2 days	6 hours	
Ionosphere – day (cm)	✔	55, 300	6 hours	1 hour	Subsequent passes uncorrelated; use larger values (6X) for ionosphere when only predicted calibrations available.
Ionosphere – night (cm)	✔	15, 100	6 hours	1 hour	
Troposphere – wet (cm)	✔	1, 1	6 hours	1 hour	S-band units.
Troposphere – dry (cm)	✔	1, 1	6 hours	1 hour	

ΔDOR measurements were acquired by having two DSN stations simultaneously observe the spacecraft followed by simultaneous observations of a reference radio source (quasar). ΔDOR measured the angular separation between the spacecraft and the quasar. The two possible pairings of DSN stations were Goldstone–Madrid and Goldstone–Canberra. The Goldstone–Madrid baseline (oriented east–west) primarily measured the right ascension component of the spacecraft, whereas the Goldstone–Canberra baseline (oriented north–south) primarily measured the declination component. ΔDOR complements Doppler and range measurements because of its orthogonality to those data types. ΔDOR measurements also are independent of geometry and do not rely on dynamic models to infer position (unlike Doppler and range). The ΔDOR observable was a phase delay time expressed in units of nanoseconds (ns) that is equivalent to an angular separation between the spacecraft and the quasar. Early in development, the ΔDOR data was to be used only for independent trajectory validation and not for primary orbit determination. This was because the ΔDOR data acquisition system, including the VLBI Science Recorders (VSRs) had just been implemented at the DSN complexes and were to be validated on the 2001 Mars Odyssey mission, which arrived at Mars in October, 2001. As the system became validated with the Odyssey experience, the Navigation Team immediately recommended its adoption as a baseline capability for MER. The error budget outlined in Table 1 was determined from undifferenced media errors, quasar locations, and thermal noise considerations by the developers of the

ΔDOR acquisition system in JPL's Tracking Systems and Applications Section.

Earth Orientation

Doppler and range data determine the position of the spacecraft with respect to the assumed locations of the tracking stations, which in turn depend on the orientation of the Earth. Whereas the long-period effects of precession, nutation, and tidal oscillations are well determined, the polar motion and rotational phase (expressed by UT1) are essentially random after only a few days. Consequently, there are a variety of measurements made to maintain the knowledge of these parameters, and improve their prediction. However, due to latencies in the data, and the stochastic nature of the process being observed, the steady-state uncertainties are only reached for points several days in the past, and are significantly less accurate at the end of the data arc.

The Earth orientation model values used by JPL navigation teams are produced by the Tracking Systems and Applications Section at JPL, based on inputs from JPL and non-JPL sources. The navigation team worked with that section to develop several upgrades to the estimation system for MER that reduced data latency by using daily UT1 and pole estimates derived from Global Positioning System data. This system and its error characteristics are described in Ref. 10. Before launch, the Earth orientation model began with a process noise of 2 cm (1σ), with 4 stochastic updates per day until 7 days before the end of the arc. At that point, the process noise was increased to 10 cm (1σ) by the end of the data arc in linear steps once per day. Despite being an improvement on previous models, the values used were general numbers based on experience rather than resulting from a specific study. Once Ref. 10 was available, the model was updated (see Table 2) with a 2-day correlation time, and increased process noise values at epochs chosen such that the resulting uncertainties matched the predicted uncertainties. Since the knowledge of UT1 degraded more quickly than that of the polar motion, the increase in UT1 uncertainty started earlier.

Station Locations

While Doppler and range data are sensitive to DSN station locations (and through them to Earth orientation), ΔDOR data are much less sensitive, due to the use of an external reference (the quasar), which corrects almost all Earth-based modeling errors, especially as the quasar-spacecraft separation decreases to zero (described in Ref. 2). However, accurate modeling of station locations is still important for deriving an accurate orbit determination solution with the ΔDOR data withheld, which is important in evaluating solution consistency. The DSN stations used by MER are located at three tracking complexes near Goldstone, CA, Madrid, Spain, and Canberra, Australia, and comprise 5, 4, and 3 antennas at each site, respectively. Station locations are developed from a combination of survey data within the DSN complex and VLBI data, primarily between complexes, but also within them. Before launch, the Navigation Team requested an all-new analysis with the most complete and recent data, updated corrections for plate tectonic motion, and double checking consistency with the inertial reference frame (precession and nutation values). The result of the station location solution is a set of coordinates and a correlated covariance, which is scaled to account for systematic effects. Typical uncertainties are 3 to 4 cm (1σ) in each direction, with correlations of about 0.6 between complexes and close to 1 within complexes.. Since the station location error was very nearly constant over the timescale of the MER cruise, and since the tracking data (even including ΔDOR data, since only 1 or 2 quasars were used in each observation session) could not improve the station location knowledge, the station location errors were one of the few consider parameters.

Range Biases

Since a range measurement is made using all of the tracking station uplink and downlink electronics, additional delays due to path length and electronic frequency response are introduced. During the pre-pass calibration, the tracking station contribution to the total delay is measured, but the result is only accurate to perhaps 0.5 m (1σ) of random error at best, with an additional constant delay of about 1 m (1σ), due to factors such as the inability of the calibration to introduce a realistic Doppler shift on the ranging signal. Pre-launch modeling used 2 m (1σ) as a per-pass bias (with no correlation from pass to pass), and no constant bias, based on then-current conservative accuracy assumptions. Since the primary effect of the range bias assumptions is on solutions that do not contain ΔDOR data, accurate range bias modeling is mainly desired to produce solution consistency, and conservatism does not degrade delivery accuracy results.

In addition to the small biases discussed above, occasionally passes would be biased by a larger amount (3 to over 10 m), primarily due to difficulties executing the pre-pass range calibration. For such passes, the per-pass bias a priori uncertainty was increased to 10 m (1σ) or more, and values were possibly corrected to be consistent to nearby passes. Regardless of the adjustment, the effect of the large

uncertainties was to keep the bias for that pass from adversely affecting the solution. The spacecraft also contributes a delay to the ranging signal, primarily due to transponder electronics. This delay is calibrated before launch and assumed to be constant. In practice, this delay does not need to be estimated due to other errors with similar appearance (e.g., the Mars ephemeris error) being present in the filter.

Transmission Media

The radio signal propagating between the tracking station and the spacecraft experiences delays due to the Earth's troposphere and ionosphere and also due to interplanetary solar plasma. The troposphere is modeled using meteorological data at the tracking complexes combined with GPS-derived estimates of the troposphere difference in the upper atmosphere. The result of the troposphere measurements is a model for zenith delay, which is then mapped to the elevation angle of each tracking measurement using the Niell mapping model. The ionosphere is calibrated by processing all available GPS data to form a global model and then evaluating the model along the ray path to each spacecraft. The interplanetary plasma can most effectively be measured with a dual-frequency signal (which MER lacked) for each spacecraft, but differences in its effect on range and Doppler data can be exploited to remove some of the effect.

The available troposphere parameters include the wet and dry components for each station complex, and the ionosphere parameters include day and night components for each complex. The remaining uncalibrated error is expressed as a combination of the two components for each media type, as shown in Tables 1 and 2. Since these errors change for each pass, they must be estimated as stochastic parameters, even though the parameter partials are only approximate. Pre-launch treatment comprised a 6-hour update time with no correlation, but this is not an especially realistic model. The measurement sensitivity to Earth media increases markedly at lower elevation angles (as is reflected in the partials), so the most important part of the model is to allow for differences between the rising and setting part of the pass. The model adopted during final approach (Table 2) used 1-hour updates with a 6-hour correlation time for each of the four Earth media parameters for each pass, with no correlation between passes. Although this model is still somewhat ad hoc, it is at least approximately realistic, and worked reasonably well for MER. Nonetheless, the Earth media estimation model would benefit from more study than the MER Navigation Team was able to devote to it.

Although range and Doppler data are affected more severely by Earth media, the ΔDOR data is not completely immune to temporal (on the timescale of scan separation) or spatial (depending on the quasar-spacecraft angular separation) errors, even after all of the differencing has been performed. The media partials are correctly computed for the ΔDOR data as well, and the parameters were treated as constants over the entire ΔDOR observation (almost always consisting of two points separated by less than an hour). Care was taken to insure that the stochastic media estimate from the Doppler and range data was not correlated with the ΔDOR media estimates, since otherwise any problems with the Doppler and range data (whether related to transmission media or not) could corrupt the ΔDOR data.

While the Earth orientation parameters display a gradual increase in uncertainty after the last data, the effect on the media calibrations is more of a step function. Consequently, after the last calibrated pass the Doppler and range tracking data were deweighted to 3 times the nominal weights (or 0.225 mm/sec (1σ) and 3 m (1σ), respectively), and the stochastic process noise was increased, to a factor of 6 for the ionosphere and a factor of 2 for the troposphere.

Spinning Spacecraft Effects

Like the Mars Pathfinder spacecraft before it, the MER spacecraft rotated at 2 rpm and had a circularly-polarized antenna with an offset from the spin axis. The removal of the sinusoidal signature from the antenna offset and the Doppler bias due to the polarized antenna is described in detail in Ref. 2, but apart from these deterministic effects there remains the possibility of an error in the magnitude of the Doppler bias. Before launch, a per-pass Doppler bias of 0.005 mm/sec (1σ) (equivalent to 0.008 rpm) was included to account for this effect, although in actuality, the Doppler bias should have been correlated on a many-day timescale, since the spin rate error would have persisted. Post-launch experience with automatic spin-signature removal was convincing enough to remove the parameter from the filter (Table 2).

Mars Ephemeris

Even though the Mars ephemeris is not related to an observation directly, the errors in the ephemeris behaved like an observation error model, since they did not interact significantly with the trajectory until within the last 2 days. All the trajectory parameters of interest are Mars-relative, so the spacecraft state at the end of the data arc is mapped to the Mars entry interface point (Mars radius equal to 3522,2 km) and to Mars periapsis. Since there was not much sensitivity to the Mars ephemeris at even the TCM-6

data cutoff (~E-13 hours), the ephemeris errors were considered for all delivered solutions.

Of course, the relative insensitivity to the Mars ephemeris depends on ephemeris errors that are similar to the current-state errors at the end of the data arc. Since the Mars Odyssey spacecraft transitioned to mapping operations in February 2002, monthly ΔDOR observations were made of both Mars Odyssey and Mars Global Surveyor. Both of these spacecraft are tied to Mars to an accuracy at least an order of magnitude better in position than the Earth-relative ΔDOR measurement accuracy. The resulting data were combined with range measurements to both spacecraft to produce an updated Mars ephemeris, which was internally delivered to the MER Navigation team as DE 410 (Ref. 11). The initial covariance (which had originally been provided with DE405+) used with this ephemeris had radial, downtrack, and normal uncertainties of 17 m, 271 m, and 884 m (all 1σ), respectively, in January 2004. However, an examination of the ΔDOR and range residuals used in the ephemeris fit strongly suggested that this covariance could be scaled down by at least a factor of two, which was the adopted value for baseline cases for final approach (Table 2). The resulting 442-m (1σ) out-of-plane uncertainty is equivalent (at the Earth-Mars range at MER arrival) to the angular error from the quasar locations (described below) or to several ΔDOR measurements being statistically combined. Treating the ephemeris errors as consider parameters statistically combined (in an RSS sense) the mapped trajectory errors with the ephemeris errors for most of the approach, and only caused additional B-plane or entry FPA uncertainty at the very end of the trajectory, when there was modest sensitivity to some of the parameters. Although included in the trajectory force model, the sensitivity to the Mars gravity field and mass errors was small, as is typically the case for hyperbolic approach trajectories Thus, errors for these parameters were not included in the filter.

Quasar Locations

The pre-launch value of 2 nrad for the locations of the quasars used for ΔDOR measurements was retained throughout the mission, although the quasars in use were probably known to 1 nrad. As the quasars are not moving appreciably in an angular sense with respect to the Earth, the quasar location errors were always considered. Since the quasar location errors were assumed to be primarily due to data noise and quasar structure, there was no correlation modeled between any of the locations. Despite the small value of the quasar location error, this error and the Mars ephemeris error became the largest consider error sources, due to the large number of ΔDOR points and the low non-gravitational acceleration uncertainty level of the spacecraft.

Spacecraft Modeling

Whereas the gravitational and relativistic acceleration on a spacecraft in interplanetary space are known almost perfectly (such that modeling the remaining errors is unimportant), the non-gravitational forces on the spacecraft are often poorly known, and are almost always the limiting factor for trajectory prediction. The MER spacecraft had very well-behaved non-gravitational accelerations, due to being a spinning spacecraft and having balanced thrusters, but the modeling of these parameters still made a significant difference in the final result. Specifically, the error modeling for solar pressure and propulsive events (attitude changes and TCMs) is described below. With the exception of the TCMs, all non-gravitational error models are included on the entire trajectory up to atmospheric entry by propagating constant errors or continuing to update stochastic parameters, instead of terminating error models at the end of the data arc.

1. Solar pressure radiation

Pre-launch modeling of solar pressure used flat plates and cylinders to model the cruise stage and to approximate the lit region of the backshell. The area of each component was estimated with a 5 percent (1σ) a priori uncertainty, and specular and diffuse reflection coefficients were estimated with an a priori uncertainty of 10 percent (1σ) of its value. An additional spherical acceleration was estimated stochastically with a 1-day update time, a 10-day correlation time, and a process noise of 2×10^{-12} km/sec^2 (1σ) to account for solar pressure errors in all three directions. However, it was recognized that both the nominal model and its errors should be updated when time permitted, which unsurprisingly turned out to be after launch.

The details of the updated solar pressure model are given in Ref. 4. Since the average surface normal vector for lit areas always fell in the Sun-spin axis plane, there was no solar pressure force out of that plane, making the acceleration modeling a two-dimensional problem. The biggest uncertainty in the model was the overall radiation balance, since any heat that did not depart through the radiators (with no net effect due to symmetry) was radiated from the top of the cruise stage instead of from the heat shield (which was always in shadow, and hence at or below −100° C), producing an additional force beyond what would be expected from the material properties of the solar arrays. The solar pressure model accounted for this effect by increasing the diffuse reflection for the flat plate representing the top of the cruise stage to a

physically unreasonable value, but one which did a good job of modeling the force for Sun-spin axis (or solar aspect) angles of about 35°. Since the solar aspect angle determined the total lit area of the spacecraft, and hence the total heat load, the cruise stage re-radiation would be expected to depend on the solar aspect angle. During Mars approach, the solar aspect angle varied between 25° and 45°, changing about half a degree per day between turns, which ranged in magnitude from 5° to 18° and occurred every 8 to 50 days.

Consequently, the solar pressure model included a stochastic diffuse reflection for the flat plate normal to the spin axis (representing the top of the cruise stage), with a process noise of 0.1 (as a coefficient), an update time of 1 day, and a 7-day correlation time. This parameter's correlation was reset at each turn, assuming that the errors would not necessarily be similar at different solar aspect angles. In addition, the specular and diffuse coefficients for each of the three components of the model (a flat plate, a cylinder for the sides of the cruise stage and aeroshell edge, and a tabular function for the lit area of the backshell) were estimated as constants with a priori sigmas of 0.1 (or 10 percent of the maximum physical coefficient value of one). In practice, the stochastic diffuse coefficient did not vary appreciably across turns, except for early in the MER-B approach where the solar aspect angle reached almost 45°, and even then the difference was less than half of the process noise. From this, it was concluded that the solar pressure model was very accurate at the approach geometry, which contributed significantly to the consistency of the approach solutions.

2. *Attitude changes*

Although spinning spacecraft can go an extended time without propulsive attitude updates, changing the spacecraft spin axis requires using thrusters and is generally required to maintain power and/or communications margins within reasonable bounds. In the case of the MER spacecraft, the attitude changes (also referred to as ACS events in Tables 1 and 2) were required to maintain communications on the medium gain antenna, but the relatively low gain of the antenna allowed the attitude changes to be correspondingly infrequent, even for a spinning spacecraft. The thruster configuration (described in more detail in Ref. 1) allows turns to be made in a balanced mode. However, because of thruster misalignments, plume impingement effects, and thruster imbalances, there was a non-zero residual ΔV resulting from ACS events. Concern with regard to the magnitude of these effects caused fairly large spherical uncertainties of 3 mm/sec (1σ) to be assumed before launch for residual ΔV from ACS events. In-flight experience with ACS event ΔV is described in a later section of this paper.

Maneuver Execution Errors

The accuracy with which a given propulsive maneuver can be executed is a function of the propulsion system behavior and the attitude control system, which maintains the pointing of the spacecraft during thruster firings. Maneuver execution errors are described in terms of components that are proportional to the commanded ΔV magnitude and components that are independent of ΔV magnitude. The MER spacecraft design was required to satisfy the maneuver execution accuracy requirements listed in Table 1 (see Comments). These values were used during pre-launch analyses and during flight operations until late in the final approach phase for *Opportunity*, at which point the values listed in Table 2 were adopted, based on accumulated experience with spacecraft performance during preceding TCMs for both *Spirit* and *Opportunity*.

Summary

Following best efforts to size the a priori errors over a several month period, we convened an additional review process in which each assumption was verified again with the originator, and another covariance analysis configuration was prepared and run by an independent navigation team member to guard against any blunders in the complex filter inputs. When these verifications were complete, the contributions of the remaining errors to the entry flight path angle delivery error were summarized in order to prioritize monitoring during cruise. These sensitivities are shown in Fig. 1 for *Spirit* at TCM-4 and TCM-5. Note that other than the loss of all Delta-DOR capability, the largest sensitivity by far was the ACS event (turn) ΔV. This emphasizes the importance of the performing an ACS/NAV calibration. When this calibration revealed the ACS ΔV to be much smaller than the a priori assumption (see below), there was good reason to believe the delivery error would be significantly improved. , This was borne out in the final delivery, which is summarized in the final section.

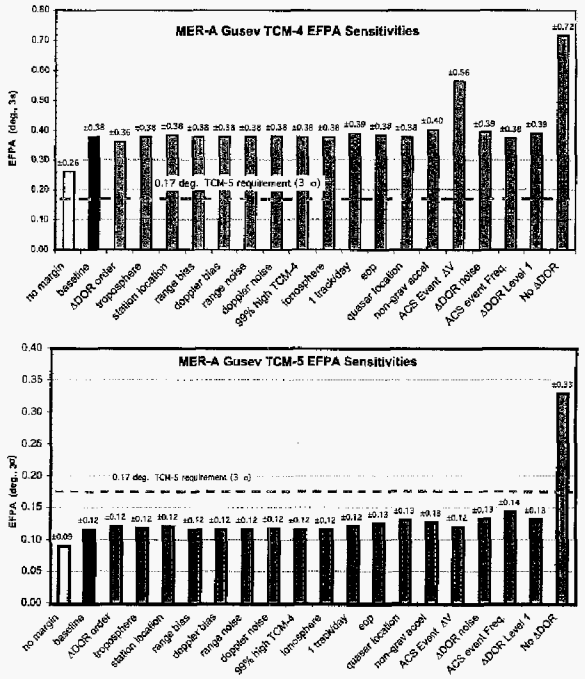

Figure 1: Entry FPA uncertainties.

III. MER Navigation Operations

Spirit was launched on a Boeing Delta II 7925 launch vehicle from Cape Canaveral Air Force Station (CCAFS) Space Launch Complex 17A (SLC-17A) on June 10, 2003, at 17:58:47 UTC on the first of two instantaneous daily launch opportunities (93° launch azimuth)

Opportunity was launched on a Boeing Delta II 7925H launch vehicle from CCAFS SLC-17B on July 8, 2003, at 03:18:15 UTC on the second of two instantaneous daily launch opportunities (99° launch azimuth).

In-flight Navigation Filter Updates and Validation

Between launch and final approach, experience with tracking data, OD solutions, and other factors caused changes to the baseline OD filter configuration. The OD filter assumptions used for the final approach phase are listed in Table 2.

First, the high quality of Doppler, range, and ΔDOR data obtained during navigation operations enabled reductions in their a priori uncertainties.

Since the ACS Event ΔV was the largest remaining pre-launch sensitivity, the ACS/NAV calibration results are discussed here in more detail. The ACS/NAV calibration activity quickly revealed that these uncertainties should be reduced from the spherical 3 mm/s (1σ) to 0.5 mm/sec (1σ) for *Spirit* and 1 mm/sec (1σ) for *Opportunity*. Further analysis of the ACS/NAV calibration showed that the unbalanced components for typical turns were 0.02 mm/sec or less except for the spin-axis component of *Opportunity* turns, which was 0.1 mm/sec. This led to the adoption of 0.05 mm/sec (1σ) as the a priori uncertainty for all components except the axial component for *Opportunity*, which was assigned an a priori uncertainty of 0.1 mm/sec (1σ) and a nominal value of 0.1 mm/sec (for typical 10° turns).

At the same time, the number of attitude turns had been cut roughly in half due to a trade between the amount of commanding activity on the spacecraft and the telecommunications performance. Although the ACS/NAV calibration had been designed for the original 5° turns, the results for 10° were not found to be twice as large, so the net result of the decrease in the number of turns was increased trajectory knowledge. For the delivery at entry, the most important turn occurred immediately after TCM-4 on each spacecraft, which was placed 8 days before entry. The effect of the reduction in the ACS event ΔV uncertainty, and to a lesser extent the reduction in the number of turns, produced B-plane delivery accuracies that were dominated by the nominal TCM execution errors, and surface delivery accuracies that were dominated by atmospheric and spacecraft aerodynamic modeling uncertainties.

Similarly, actual spacecraft TCM performance permitted reductions in the assumed values for maneuver execution errors. The stochastic nongravitational acceleration model was eliminated from the filter in favor of upgrades to the solar pressure model. The recommended uncertainties for the Mars ephemeris and Earth orientation parameters (EOP) were updated. Additionally, new solutions were delivered for station locations and their uncertainties (Ref. 12). Finally, the Doppler bias model was eliminated, because the observed biases were very small, and the updated station locations further decreased the usefulness of including a Doppler bias in the filter model. Overall, during navigation operations, orbit determination performance improved significantly from that based on pre-launch covariance studies.

Navigation Results

Prior to launch, the required atmospheric entry FPA delivery accuracies at TCM-5 (E – 2 days) were ±0.12° (3σ) for *Spirit* and ±0.14° (3σ) for *Opportunity*. Actual delivered navigation performance significantly exceeded these requirements. The OD knowledge at the time TCM-5 was canceled was ±028° (3σ) for *Spirit* and ±0.035° (3σ) for *Opportunity*. The actual errors in entry FPA, based on the final pre-entry OD solutions, were estimated to be –0.007° for *Spirit* and +0.030° for *Opportunity*. (The entry FPA error for *Opportunity* would have been much smaller had TCM-B5 not been canceled to eliminate what was judged an unnecessary correction to the predicted landing location). These FPA errors correspond to errors in the magnitude of the B-vector of only 180 m for *Spirit* and 750 m for *Opportunity*. Navigation performance for *Spirit* was such that only four of six planned TCMs were required; TCMs A5 (E – 2 days) and A6 (E – 4 hours) were canceled. For *Opportunity*, only three of six planned TCMs were required; TCMs B3 (E – 65 days), B5 (E – 2 days) and B6 (E – 4 hours) were canceled.

Landing accuracy was also exemplary. Figs. 2 and 3 show the landing target, final pre-entry estimated landing points and associated 99% dispersion ellipses, and actual landing locations for *Spirit* and *Opportunity*. The miss distances from the target landing point, caused solely by navigation errors at atmospheric entry, were only 3.3 km (uptrack) for *Spirit* and 9.7 km (downtrack) for *Opportunity*. Total miss distances, including errors introduced from atmosphere and spacecraft aerodynamics uncertainties, were 10.1 km (mostly downtrack) for *Spirit* and 24.6 km (downtrack) for *Opportunity*. These mostly along-track surface miss distances should be compared to the end-to-end lengths of the 99% probability target landing ellipses: 67 km (unmargined) or 78 km (margined) for *Spirit* and 74 km (unmargined) or 85 km (margined) for *Opportunity*.

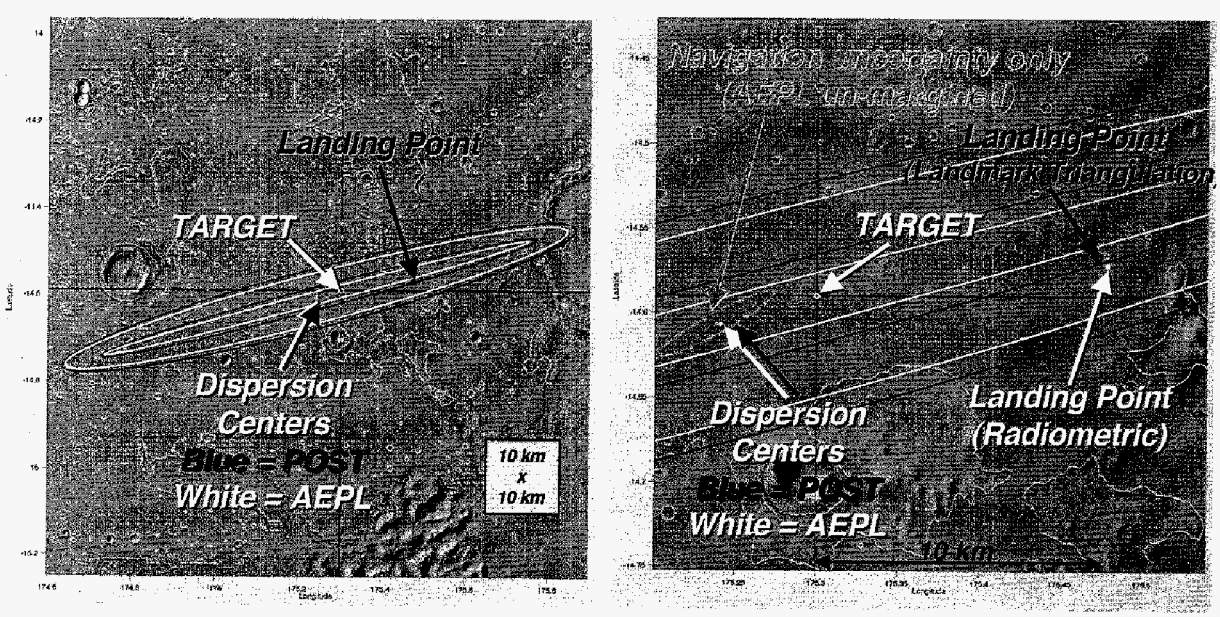

Figure 2: *Spirit* final pre-entry landing estimate and actual landing location.

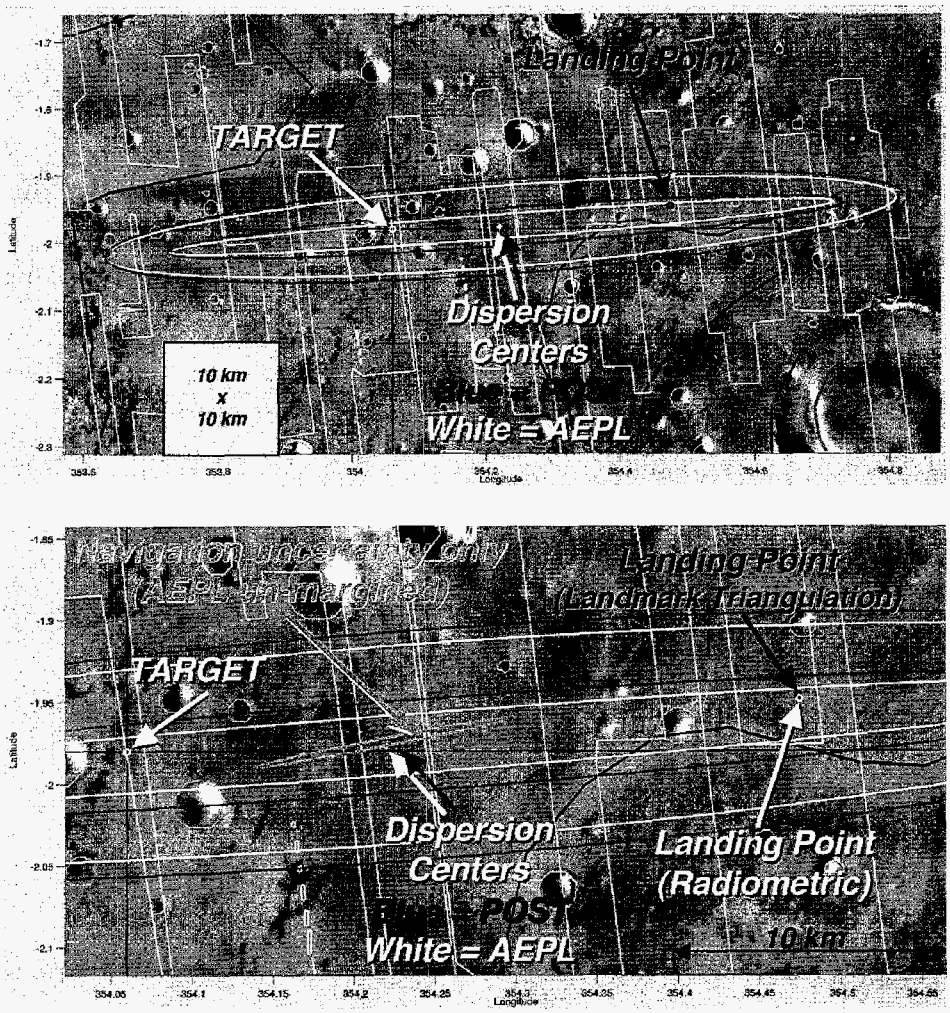

Figure 3: ***Opportunity*** **final pre-entry landing estimate and actual landing location.**

IV. Conclusion

The system developed for navigating the two MER spacecraft to Mars was significantly improved relative to prior Mars missions. These improvements enabled the selection of high science value landing sites and were necessary to the meet the stringent atmospheric entry delivery requirements in order to yield landing dispersions that were small enough to ensure a high probability of a safe landing for both the *Spirit* and *Opportunity* landers. The deep understanding of the navigational error budget and the methods used for navigation and validation for MER will serve as a new standard for all future Mars landers and interplanetary missions.

Acknowledgments

The outstanding MER navigation results presented in this paper are the direct result of the efforts of a large group of people, including the following: Timothy McElrath, Christopher Potts, Darren Baird, Eric Graat, Brian Portock, and Geoff Wawrzyniak, Behzad Raofi, Julie Kangas, Philip Knocke, Ralph Roncoli and Prasun Desai, Lynn Craig, Joseph Guinn, Shyam Bhaskaran, Tomas Martin-Mur, Kevin Criddle, Earl Higa, and Neil Mottinger, Laura Campanelli, Lorena Carrillo, K. J. Lee, and Teresa Thomas, Peter Antreasian, Amy Attiyah and Ron Baalke, Brian Kennedy, Victor Legerton, Daniel Lyons, Dimitri Gerasimatos Jean Patterson and James Border, Moriba Jah and Michael Wilson, Walid Majid, Sumita Nandi, and Elizabeth Quintanilla, and, lastly, the members of the

Navigation Advisory Group of the Navigation and Mission Design Section. This research was carried out at the Jet Propulsion Laboratory, California Institute of Technology, under a contract with the National Aeronautics and Space Administration.

Reference herein to any specific commercial product, process, or service by trade name, trademark, manufacturer, or otherwise, does not constitute or imply its endorsement by the United States Government or the Jet Propulsion Laboratory, California Institute of Technology.

References

[1]D'Amario, L. A., "Mars Exploration Rovers Navigation Results," *AIAA/AAS Astrodynamics Specialist Conference*, AIAA-2004-4980, AIAA, Washington, DC, 2004.

[2]Portock, B. M., Graat, E. J., McElrath, T. M., Watkins, M. M., and Wawrzyniak, G. G., "Mars Exploration Rovers Cruise Orbit Determination," *AIAA/AAS Astrodynamics Specialist Conference*, AIAA-2004-4981, AIAA, Washington, DC, 2004.

[3]McElrath, T. P., Watkins, M. M., Portock, B. M., Graat, E. J., Baird, D. T., Wawrzyniak, G. G., Guinn, J. R., Antreasian, P. G., Attiyah, A. A., Baalke, R. C., and Taber, W. L., "Mars Exploration Rovers Orbit Determination Filter Strategy," *AIAA/AAS Astrodynamics Specialist Conference*, AIAA-2004-4982, AIAA, Washington, DC, 2004.

[4]Wawrzyniak, G. G., Baird, D. T., Graat, E. J., McElrath, T. P., Portock, B. M., and Watkins, M. M., "Mars Exploration Rovers Orbit Determination System Modeling," *AIAA/AAS Astrodynamics Specialist Conference*, Providence, AIAA-2004-4983, AIAA, Washington, DC, 2004.

[5]Kangas, J. A., Potts, C. L., and Raofi, B., "Mars Exploration Rovers Launch Performance and TCM-1 Maneuver Design," *AIAA/AAS Astrodynamics Specialist Conference*, AIAA-2004-4984, AIAA, Washington, DC, 2004.

[6]Potts, C. L., Raofi, B., and Kangas, J. A., "Mars Exploration Rovers Propulsive Maneuver Design," *AIAA/AAS Astrodynamics Specialist Conference*, AIAA-2004-4985, AIAA, Washington, DC, 2004.

[7]Baird, D. T., McElrath, T. P., Portock, B. M., Graat, E. J., Wawrzyniak, G. G., Knocke, P. C., D'Amario, L. A., Watkins, M. M., Craig, L. E., and Guinn, J. R., "Mars Exploration Rovers Entry, Descent, and Landing Navigation," *AIAA/AAS Astrodynamics Specialist Conference*, AIAA-2004-5091, AIAA, Washington, DC, 2004.

[8]Desai, P. N., and Knocke, P. C., "Mars Exploration Rovers Entry, Descent, and Landing Trajectory Analysis," *AIAA/AAS Astrodynamics Specialist Conference*, AIAA-2004-5092, AIAA, Washington, DC, 2004.

[9]Knocke, P. C., Wawrzyniak, G. G., Kennedy, B. M., Parker, T. J., Golombek, M. P., Duxbury, T. C., Kass, D. M., and Desai, P. N., "Mars Exploration Rovers Landing Dispersion Analysis," *AIAA/AAS Astrodynamics Specialist Conference*, AIAA-2004-5093, AIAA, Washington, DC, 2004.

[10]Ratcliff, J. T., "KEOF Operational EOP Deliveries During MER," 24 July 2003 (JPL internal memo).

[11]Standish, E. M., "Recommendation of DE410 for MER and Cassini," 3 November 2003 (JPL internal memo)..

[12]Folkner, W. M. and Jacobs, C. S., "DSN Station Location Update for MER," 4 November 2003 (JPL internal memo).